

Additional Volumes in Preparation

Power System Modeling, Analysis, and Control, A. P. Sakkis Melo-poulos

High Voltage Circuit Breakers, Ruben Garzon

Integrating Electrical Heating Elements in Appliance Design, Thor Hegbom

Magnetic Core Selection for Transformers and Inductors: A User's Guide to Practice and Specification, William T. McLyman

Permanent Magnet Motor Technology

Design and Applications

Jacek F. Gieras
Mitchell Wing
University of Cape Town
Rondebosch, South Africa

Marcel Dekker, Inc.

New York•Basel•Hong Kong

Fig. 7.9 shows a schematic of the disk type 8-pole prototype micromotor with etched winding [85]. The dimensions of the NdFeB PM are: thickness 3 mm, outer diameter 32 mm and inner diameter 9 mm. Although the stator laminated core reduces losses, it is difficult to manufacture. It was decided to design a four layer etched stator winding (Fig. 7.9b). The current conducting path has a width of 0.4 mm and a thickness of 0.1 mm. The electric time constant of the stator winding per phase is $L_1/R_1 = 0.7 \mu\text{s}$. The four phase stator winding is fed by four transistors. Magneto resistive position sensors have been used. The sensor PM has the dimensions $3 \times 3 \times 1$ mm. The torque of 0.32 mNm at a speed of 1000 rpm and input voltage 3.4 V has been developed.

7.4.2 Micromotors of cylindrical construction

Cylindrical brushless micromotors can be designed both as synchronous and d.c. micromotors, depending on the electronic control system. Usually, two-phase, 2-pole or 4-pole cylindrical brushless micromotors are designed. The electromagnetic torque-to-armature current ratio is from $2 \times 10^{-7} \text{ Nm/A}$ to $7 \times 10^{-7} \text{ Nm/A}$ [86]. Construction examples are shown in Fig. 7.10 [86]. The stator armature coils consist of a few turns of flat copper wire (typical thickness 35 μm).

7.5 Axial flux motors

The axial flux PM motor is an attractive alternative to the cylindrical radial flux motor due to its short frame, compact construction and high power density. These motors are particularly suitable for pumps, fans, robots and electrical automobiles. They have become widely used for low-torque servo and speed control applications [107]. Axial flux or disk-type PM motors can be designed as double-sided or single-sided machines, with or without armature slots, with internal or external PM rotors and with surface mounted or interior type PMs. Low power axial flux PM machines are usually machines with slotless windings and surface PMs.

In some cases, rotors are actually embedded in power-transmission components to optimize mass, assembly time and power transfer. In the case of electric buses with built-in wheel motors the payoff is higher efficiency and lower cost. Dual-function rotors may also appear in pumps and other types of machinery, bringing new levels of performance to these products.

The control of axial flux disk rotor motors is identical to that of PM off a.c. mains or as a brushless d.c. motor using power electronics. The

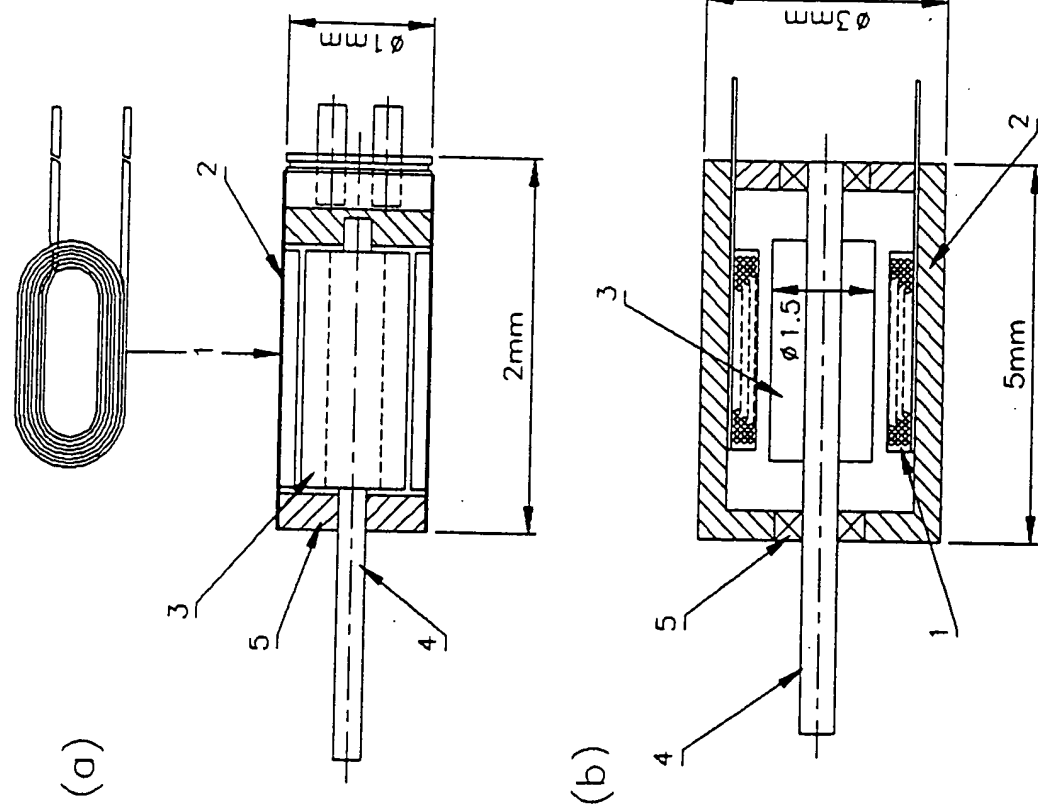


Figure 7.10: Construction of cylindrical brushless PM micromotors: (a) synchronous micromotor designed at Eindhoven University of Technology, Netherlands, (b) 4-mW, 2-V micromotor designed by Toshiba Co. 1 — stator coil, 2 — bearing, 3 — stator yoke, 4 — rotor magnet, 5 — stainless steel shaft, 5 — bearing.

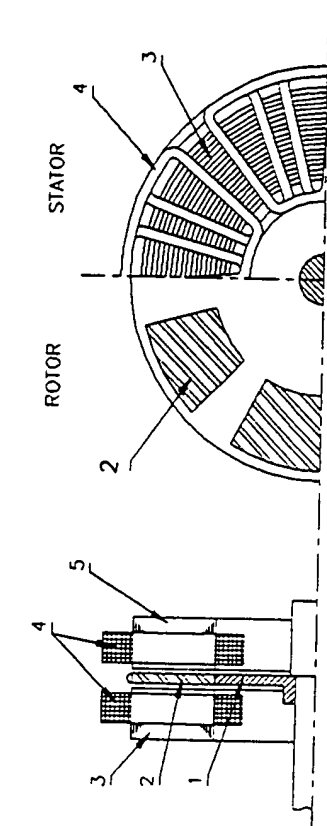


Figure 7.11: Configuration of double-sided PM synchronous motor with internal disk rotor: 1 — rotor, 2 — PM, 3 — stator core, 4 — stator winding.

majority of application use the disk-type motor as a brushless d.c. motor. Power electronic transistor switches are used to control the flow of current in the windings according to the rotor position to ensure maximum torque. Rotor position sensors are thus a vital part of the brushless d.c. disk motor.

In the design and analysis of axial flux motors the topology is complicated by the presence of two airgaps, high axial attractive forces, changing dimensions with radius and the fact that torque is produced over a continuum of radii, not just at a single radius as in cylindrical motors.

The calculation of the winding inductances and induced EMF can be done using a three-dimensional FEM. The magnetic model can be simplified to a two-dimensional model by introducing a cylindrical cutting plane at the mean radius of the magnets [68]. This axial section is unfolded into a two-dimensional surface on which the finite element analysis can be done, as discussed for cylindrical PM motors in Chapters 3 and 5.

7.5.1 Double-sided motor with internal PM disk rotor

In the *double-sided motor with internal PM disk rotor*, the armature winding is located on two stator cores. Normally, the stator cores are wound from electrotechnical steel strip and the slots are machined by shaping or planing.

Another method is first to punch the slots with variable distances between them and then to wind the steel strip into the form of the slotted toroidal core. Such a manufacturing process has been implemented by the R & D Institute of Electrical Machines VUES in Brno, the Federal Republic

of Czech. This manufacturing process also allows for making skewed slots to minimize the effect of slot harmonics. Each stator core has skewed slots in opposite direction. It is recommended to make a wave stator winding to obtain shorter end connections and more space for the shaft. The *R & D Institute of Electrical Machines* in Brno also proposes an odd number of slots, e.g. 25 instead of 24 to reduce the torque ripple.

The disk with PMs rotates between two stator cores. An eight-pole configuration is shown in Fig. 7.11. PMs are embedded or glued in a nonferromagnetic rotor skeleton. The nonferromagnetic airgap is large, i.e. the total airgap is equal to two mechanical clearances plus the thickness of a PM with μ_r close to unity. A double-sided motor with parallel connected stators can operate even if one stator winding is broken. A series connection, however, can provide equal opposite axial attractive forces.

The main dimensions of double-sided PM synchronous motors with internal disk rotors can be found on the following assumptions: (a) the phase windings of two stators are connected in parallel, (b) the number of turns per phase per one stator is N_1 , (c) the phase armature current in one stator winding is I_a .

The line current density per one stator is expressed by eqn (5.10) in which the inner stator diameter should be replaced by an average diameter $D_{av} = 0.5(D_{ext} + D_{in})$ (7.7)

where D_{ext} is the external diameter of the stator and D_{in} is the internal diameter of the stator (Fig. 7.11). The pole pitch and the effective length of stator core in radial direction are:

$$\tau = \frac{\pi D_{av}}{2p} \quad L_i = 0.5(D_{ext} - D_{in}) \quad (7.8)$$

The EMF induced in the stator winding by the rotor excitation system, according to eqn (5.4), for the disk rotor synchronous motor has the following form:

$$E_f = \pi\sqrt{2}n_s p N_1 k_w \Phi_f = \pi\sqrt{2}n_s N_1 k_w D_{av} L_i B_{mg} \quad (7.9)$$

where the magnetic flux

$$\Phi_f \approx \frac{2}{\pi} \tau L_i B_{mg} = \frac{D_{av}}{p} L_i B_{mg} \quad (7.10)$$

The electromagnetic power in two stators

$$S_{etm} = m_1 E_f / (2I_a) = \pi^2 k_w D_{av}^2 L_i n_s B_{mg} A_m \quad (7.11)$$

It is convenient to use the ratio of external-to-internal stator diameter

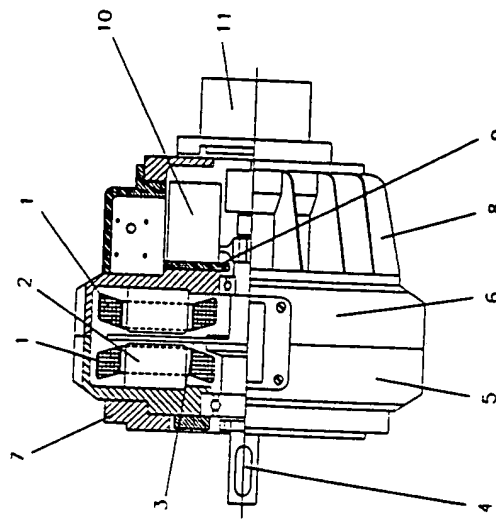


Figure 7.12: Double-sided axial flux motor with built-in brake: 1 — stator winding, 2 — stator core, 3 — disk rotor with PMs, 4 — shaft, 5 — left frame, 6 — right frame, 7 — flange, 8 — brake shield, 9 — brake flange, 10 — electromagnetic brake, 11 — position sensor. Courtesy of SVST Bratislava, Slovakia.

7.5.2 Double-sided motor with internal stator

A double-sided motor with internal stator is more compact than the previous construction with internal PM rotor [69, 173, 200]. In this machine the toroidal stator core is formed from a continuous tape. The polyphase slotless armature winding is located on the surface of the stator core. The total airgap is equal to the thickness of the armature winding, mechanical clearance and the thickness of the PM in the axial direction. The double-sided rotor with PMs is located at two sides of the stator. The configuration is shown in Fig. 7.13 [173].

Owing to the large airgap the maximum flux density does not exceed 0.6 T. To produce this flux density a large volume of PMs is required. Since the permeance component of the flux ripple associated with the slots is eliminated the vibration of electromagnetic nature is absent. The magnetic circuit is unsaturated (slotless stator core). On the other hand, the machine structure lacks the necessary robustness.

The stator can also be made with slots (Fig. 7.14). For this type of motor slots are progressively notched into the steel tape as it is passed from one mandrel to another and the polyphase winding is inserted [200]. In the case of the slotted stator the airgap is small ($g \leq 0.5$ mm) and the airgap magnetic flux density increases to 0.85 T [69]. The magnet thickness is less than 50% of the previous design (Fig. 7.13).

There are a number of applications for large disk motors with external PM rotors, especially in electrical vehicles [69, 200]. Disk-type motors with external rotors have particular advantage in low speed high torque applications, such as buses and shuttles, due to their large radius for torque production. For small electric cars, the possibility of mounting the electric motor directly into the wheel has many advantages; it simplifies the drive system and the constant velocity joints are no longer needed [69].

$$k_d = \frac{D_{ext}}{D_{in}} \quad (7.12)$$

The parameter $D_{av}^2 L_i$ proportional to the volume of one stator is

$$D_{av}^2 L_i = \frac{1}{8} \left(1 + \frac{1}{k_d}\right) \left(1 - \frac{1}{k_d^2}\right) D_{ext}^3 \quad (7.13)$$

Putting

$$k_D = \frac{1}{8} \left(1 + \frac{1}{k_d}\right) \left(1 - \frac{1}{k_d^2}\right) \quad (7.14)$$

the volume of one stator is proportional to $D_{av}^2 L_i = k_D D_{ext}^3$. In connection with eqn (5.60) the stator external diameter is

$$D_{ext} = \sqrt[3]{\frac{\epsilon P_{out}}{\pi k_w k_D n_s B_{mg} A_m \eta \cos \theta}} \quad (7.14)$$

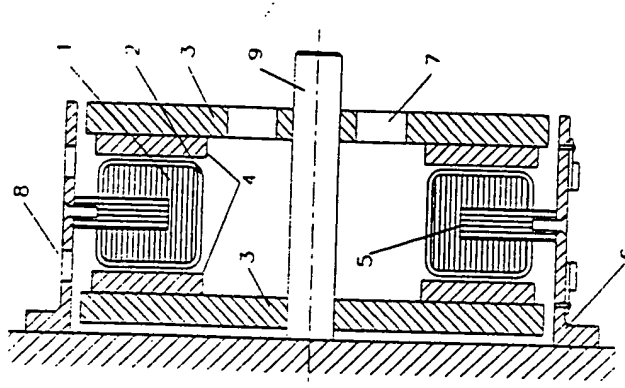


Figure 7.13: Double-sided motor with internal slotless stator: 1 — stator frame, 2 — stator winding, 3 — disk, 4 — PMs, 5 — peg, 6 — stator frame, 7 — air outlet, 8 — air inlet, 9 — shaft.

7.5.4 Multidisk motors

Multidisk motors are described e.g. in papers [1, 41]. A 300-kW, 750-Hz, 9000-rpm prototype motor with three disk rotors and two wound stators has a water cooling system with radiators around the winding end connections [41]. To minimize the winding losses the cross section of conductors is bigger in the slot area (skin effect) than in the end connection region. Using a variable cross section means a gain of 40% in the rated power [41]. SmCo PMs of trapezoidal shape ($2p = 10$) have been placed in rotor cavities and fixed with glue. Owing to high mechanical stresses the disk rotors have been made of titanium alloy.

A study of optimization of multidisk PM synchronous machines is given in the paper [1].

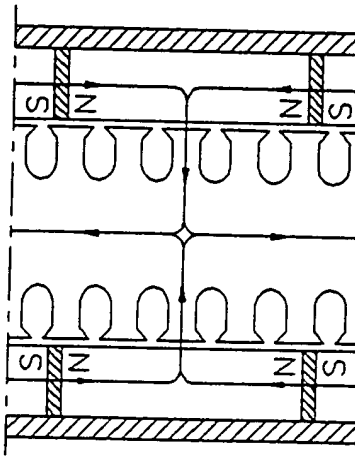


Figure 7.14: Double-sided motor with internal slotted stator and buried PMs.

7.6 Three-axis torque motor

The *three-axis torque motor* can be designed as a PM or reluctance spherical motor. It can be used e.g. in air-borne telescopes. This motor has double-